ORIGINAL PAPER

Adsorption of some cationic and anionic dyes on magnetite nanoparticles-modified activated carbon from aqueous solutions: equilibrium and kinetics study

Tayyebeh Madrakian · Abbas Afkhami · Hediye Mahmood-Kashani · Mazaher Ahmadi

Abstract   In this study, magnetite nanoparticles-modified low-cost activated carbon (MMAC) was used as an adsorbent for the removal of the anionic and cationic dyes Congo red, reactive blue 19, thionine, janus green B, methylthymol blue and mordant Blue 29, from aqueous solutions. Batch studies were performed to address various experimental parameters like pH, contact time, temperature and adsorbent dosage for the removal of these dyes. Kinetic studies showed that the adsorption of dyes on MMAC was a rapid process. Quasi equilibrium was reached in 30 min. Pseudo-first order and pseudo-second order models were used to fit the experimental data. Pseudo-second order rate equation was able to provide realistic description of adsorption kinetics. Equilibrium isotherms were analyzed by Freundlich, Langmuir, Redliche–Peterson (R–P) and Sips equations using correlation coefficients and RMS error function. Sips equation is found to best represent the equilibrium data for dye–MMAC system. It was clear that affinity of synthesized adsorbent to cationic dyes is much higher than anionic dyes.

Keywords   Cationic dyes · Anionic dyes · Magnetite-modified activated carbons · Adsorption · Removal

Introduction

At present, there are more than 1×10^5 commercial dyes with a rough estimated production of 7×10^5–1×10^6 tons per year [1]. Of such a huge production, the exact data on the quantity of dyes discharged in the environment are not available. However, it is reported that 10–15 % of the used dyes enter the environment through wastes [2, 3]. The big consumers of dyes are textile, dyeing, paper and pulp, tannery and paint industries, and hence the effluents of these industries as well as those from plants manufacturing dyes tend to contain dyes in sufficient quantities. Dyes are considered an objectionable type of pollutant because they are toxic [4, 5] generally due to oral ingestion and inhalation, and lead to problems like skin and eye irritation, skin sensitization which might also be due to carcinogenicity [5–7]. They impart color to water which is visible to human eye and therefore is highly objectionable on esthetic grounds. Not only this, they also interfere with the transmission of light and disturb the biological metabolism processes which cause the destruction of aquatic communities present in the ecosystem. Further, the dyes have a tendency to sequester metal and may cause micro-toxicity to fish and other organisms [1]. As such, it is important to treat colored effluents for the removal of dyes.

Many treatments have been investigated [the methodologies classified generally adopted to treat dye wastewater in four categories: (i) physical (ii) chemical (iii)biological and (iv) acoustical, radiation, and electrical processes] regarding their effectiveness in either removing the dyes from dye-containing effluent, or decolorizing dyes through liquid fermentations [8].The adsorption process has an edge over the other treatment methods due to its sludge-free operation and complete removal of dyes even from dilute solutions. Adsorption is one of the processes, which besides being widely used for dye removal also has a wide applicability in wastewater treatment [9–12]. Dyes that are difficult to biological breakdown can often be removed using the adsorbents. A good adsorbent [13, 14] should generally possess a porous structure (resulting in high surface area)

T. Madrakian (✉) · A. Afkhami · H. Mahmood-Kashani · M. Ahmadi
Faculty of Chemistry, Bu-Ali Sina University, Hamedan, Iran
e-mail: madrakian@gmail.com

and the time taken for the adsorption equilibrium to be established should be as small as possible so that it can be used to remove dye wastes in lesser time. Some of the adsorbents, which are generally used for dye wastewater treatment, are: alumina [15], silica gel [16], zeolites [17], activated carbon [18], metal oxides [19] and etc.

Activated carbon is the most widely used adsorbent for dye removal. It is the oldest adsorbent known and is usually prepared from coal, coconut shells, lignite, wood etc., using one of the two basic activation methods: physical and chemical [1]. Activated carbon normally has a very porous structure with a large surface area ranging from 500 to 2,000 $m^2 g^{-1}$ [20]. It has been found that adsorption on activated carbon is not usually selective as it occurs through van der Waals forces. The activated carbons, which are used as adsorbents, remove not only different types of dyes [21–23] but also other organic and inorganic pollutants such as metal ions, phenols, pesticides, chlorinated hydrocarbon, humic substances, detergents, organic compounds which cause taste and odor and many other chemicals and organisms [1]. It is well known that adsorption by activated carbon is an effective and commercially applicable method for removing color and other pollutants from textile and dye wastes. Porter [24] suggested that carbon adsorption is a complete treatment for textile water. McKay [25] used activated carbon of Filtrasorb type for the removal of acidic, basic, disperse and direct dyes and found it to be excellent for the removal of all except direct dyes. Walker and Weatherly [26] studied the kinetics of acid dye, tectilon red 2B, on GAC. The adsorption of three reactive dyes used in textile industry on Filtrasorb 400 activated carbon was studied by Al-Degs et al. [27] and the same authors [21] further studied various activated carbons for the removal of cationic dye (methylene blue) and anionic dye (reactive black), and reported that there exists a good relationship between the performance of activated carbons and methylene blue capacity/surface area.

Although activated carbon removes dyes from the solution, they are then present in a more concentrated and toxic form, and so their safe disposal increases the costs further. Therefore, the potential exists for the process of dye removal by adsorption to be more economically feasible by looking at the use of magnetic nanoparticle-loaded adsorbents [28, 29].

The present study focuses attention on the adsorption of cationic and anionic dyes [Congo red (CR), reactive blue 19 (RB), thionine (Th), janus green B (JG), methylthymol blue (MTB) and mordant blue 29 (MOB)] on activated carbon and for facility in the filtration; activated carbon was loaded with magnetite nanoparticles. Conditions of maximum adsorption were evaluated in this study, besides fitting the adsorption data to various equations to obtain certain constants related to the adsorption phenomena.

Experimental

Instrumentation

A Metrohm model 713 pH meter was used for pH measurements. A single beam UV-mini-WPA spectrophotometer was used for the determination of dye concentration in the solutions. The size, morphology and structure of the nanoparticles were characterized by transmission electronic microscopy (TEM, Philips, CM10, 100 kV) and scanning electron microscope (SEM-EDX, XL30, Philips, the Netherlands). The crystal structure of synthesized materials was determined by an X-ray diffractometer [XRD, 38066 Riva, d/G. Via M. Misone, 11/D (TN) Italy] at ambient temperature.

Reagents and materials

All chemicals were of analytical reagent grade or the highest purity available from Merck Company (Darmstadt, Germany), and double distilled water (DDW) was used throughout the study. In addition, all glasswares were soaked in dilute nitric acid for 12 h and finally rinsed for three times with DDW prior to use. Stock solutions of dyes were prepared by dissolving the powder in DDW. Dye solutions of different initial concentrations were prepared by diluting the stock solution in appropriate proportions.

Preparation of the adsorbent

Activated carbon was first dispersed in concentrated nitric acid at 130 °C for 30 min under stirring to remove the impurities and then washed by DDW until the filtrate was neutral. The purified activated carbon (1.0 g) was suspended in distilled water (125 mL). A ferric–ferrous chloride solution was freshly prepared by adding 11.68 g $FeCl_3 \cdot 6H_2O$ and 4.3 g $FeCl_2 \cdot 4H_2O$ to distilled water (125 mL) and the solution was vigorously stirred at 85 °C. The suspension formed was then added into an aqueous suspension of activated carbon at room temperature and sonicated for 30 min. After mixing, 20 mL of 30 % NH_3 solution was added drop wise into the suspension until the pH raised to 10–13. During NH_3 addition, the suspension became dark brown at pH ∼ 6 and then black at pH ∼ 11. After mixing for 60 min, the suspension was aged at room temperature for 24 h and then repeatedly washed with distilled water followed by ethanol. The magnetite nanoparticles-modified low-cost activated carbon (MMAC) was magnetically filtered and dried overnight at 50 °C in a hot air oven (Fig. 1).

Dye removal experiments

Batch sorption studies were conducted to obtain rate and equilibrium data at different temperatures and adsorbent dosages in order to construct equilibrium isotherms. In the equilibrium studies, solution pH and temperature were adjusted. Adsorption studies were performed by adding 0.03 g MMAC to 20 mL solution of different concentrations of dyes in a 50 mL beaker and the solution was stirred for 30 min. Then the dye-loaded MMAC was separated with magnetic decantation. The concentration of dye in the solution was measured spectrophotometrically at the wavelength of the maximum absorbance of each dye. The concentration of dyes decreased with time due to their adsorption by MMAC. The adsorption percent for dye, i.e., the dye removal efficiency, was determined using the following expression:

$$\%Re = \left[\frac{(C_0 - C_t)}{C_0}\right] \times 100 \qquad (1)$$

where C_0 and C_t represent the initial and final (after adsorption) concentration of dye in mg L^{-1}, respectively.

Dye uptake q (mg dye per gram of MMAC) was determined by mass balance, as follows:

$$q_t = (C_0 - C_t) \times \frac{V}{m} \qquad (2)$$

where V is the volume of the solution (L), and m is the mass of MMAC (g).

Results and discussion

Characterization of the adsorbent

The SEM of the pretreated activated carbon and MMAC and TEM image of MMAC, as shown in Figs. 2 and 3, revealed that the surface of activated carbon was modified with magnetite nanoparticles and gave it magnetic properties. The XRD profiles of pretreated activated carbon, magnetite and MMAC are shown in Fig. 4. From the XRD profile of MMAC shows, the typical peaks of Fe_3O_4 can be observed. The results confirm that Fe_3O_4 nanoparticles are successfully impregnated onto activated carbon particles.

Figure 4a and b shows the XRD profiles for AC and magnetite, respectively. The typical peaks of magnetite at $2\theta = 30.2^o$, 35.6^o, 43.3^o and 57.2^o are observed that can be assigned to magnetite [36]. Fig. 4c shows the XRD profile for MMAC that includes all the AC and magnetite nanoparticles peaks. The results confirm that iron oxide nanoparticles are adsorbed on the surface of AC.

Effect of initial solution pH on dye uptake

Solution pH affects adsorption process of dye molecules by both aqueous chemistry and surface binding sites of the adsorbent. The effect of pH in the range 3.0–10.0 with a stirring time of 45 min on the removing of dyes was investigated using 0.1 mol L^{-1} HCl or NaOH solutions for pH adjustment, with the initial dye concentration fixed at 20.0 mg L^{-1}. Figure 5 shows the removal efficiency variations as a function of pH for each dye. The adsorption percentage in the case of cationic dyes Th and JG increases with the increasing pH, reaches maximum at pH 6.0 and 9.0, respectively, and remains nearly constant at higher pHs. For anionic dyes, CR, RB, MTB and MOB, the maximum adsorption occurred at pH 4.0. Therefore, pH 9.0 was selected for cationic dyes and pH 4.0 was chosen for anionic dyes.

The point of zero charge, pH_{pzc}, of MMAC in aqueous solution was found to be 6.4, and negative zeta potential increased with increasing alkaline solution pH. In other words, the predominant charge on the MMAC at acidic pHs is positive, and because of anionic dye species, the dominant mechanism of the adsorption seems to be electrostatic attraction [28]. At pH 4.0 and below, a considerable high

Fig. 1 Photograph of MMAC adsorption behavior and magnetic separation: the suspension of the solution of CR solution and MMAC adsorbent (**a**) and removed solution of CR and separation of the MMAC adsorbent from solution with magnet after 45 min reaction (**b**)
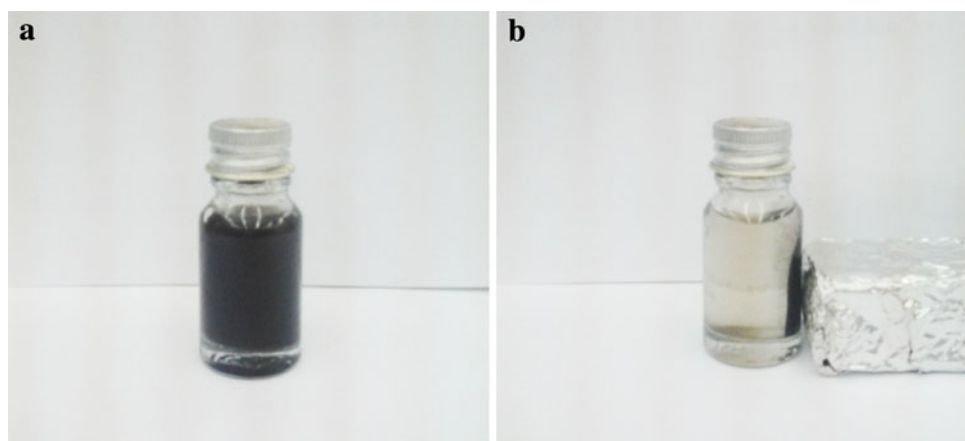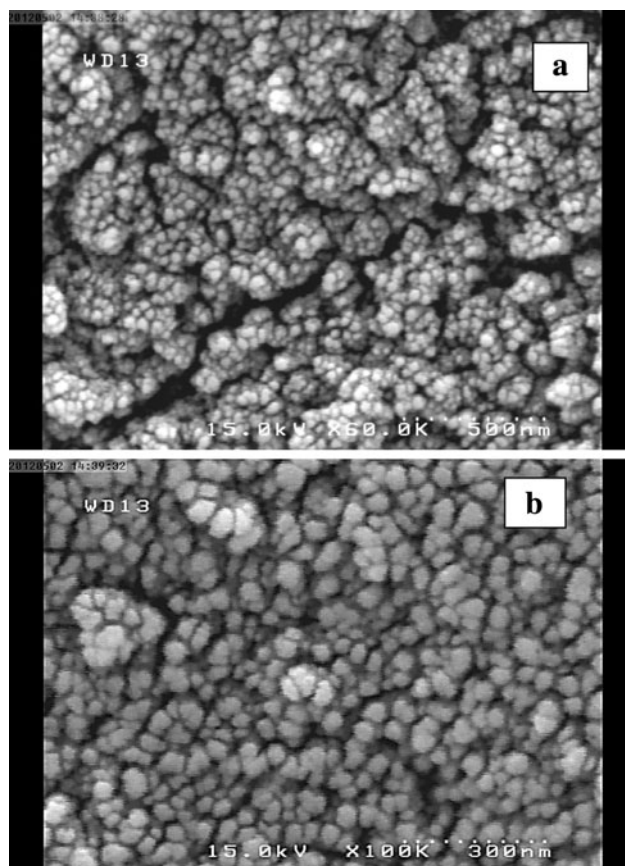
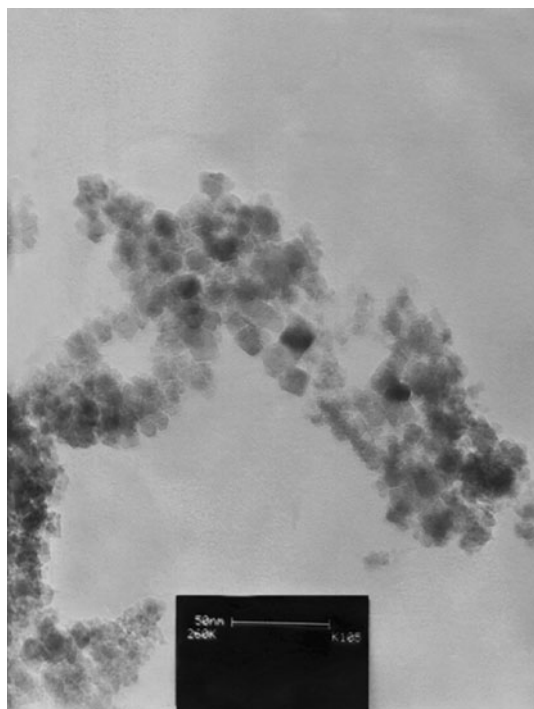Fig. 2 The SEM image of **a** AC, **b** MMAC

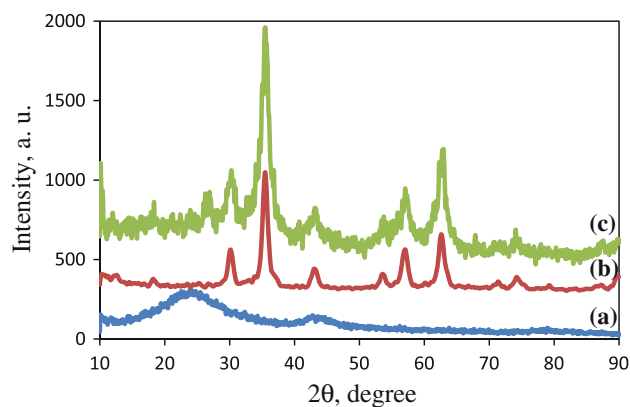Fig. 3 The TEM images of MMAC

Fig. 4 X-ray diffraction patterns of **a** AC, **b** Fe_3O_4 and **c** MMAC

electrostatic attraction exists between the positively charged surface of the adsorbent and negatively charged anionic dye molecules. By increasing the pH of the solution, the adsorption of anionic dyes on MMAC tends to decrease, which can be explained by the increasing electrostatic repulsion between the anionic dye adsorbate species and negatively charged adsorbent surfaces. In the case of cationic dyes, a similar behavior, but in the opposite direction, was observed. The lower adsorption at alkaline pHs due to the presence of excess OH^- ions destabilizing anionic dye and competing with the dye anions for the adsorption sites was observed.

Effect of adsorbent dosage on dye adsorption

The dependence of the adsorption of dye on the amount of MMAC was studied at room temperature and at optimum pH for each dye by varying the adsorbent amount from 0.01 to 0.04 g in contact with 20 mL solution of 20.0 mg L^{-1} of dye. Apparently, the percentage removal of dye increased by increasing the amount of MMAC due to the greater availability of the adsorbent. The adsorption reached a maximum with 0.03 g of adsorbent for cationic dyes and 0.04 g of adsorbent for other dyes; the maximum percentage removal was about 98 %.

Effect of contact time

The effect of contact time on the adsorption of dyes was studied to determine the time taken by MMAC to remove 20.0 mg L^{-1} dye solution at optimum pH. An optimum value of MMAC for each dye was added into a 20 mL of dye solution. Absorbance of the solution at λ_{max} with time was determined to monitor the dye concentration. It was observed that almost all the dye became adsorbed after 30 min. Therefore, agitation time of 30 min was selected for further works.

Fig. 5 Percentage of dye removal at different pHs for CR, JG, MOB, MTB, RB and Th. Conditions: 0.01 g of MMAC, 20 mL of 20.0 mg L^{-1} of dye, agitation time of 45 min
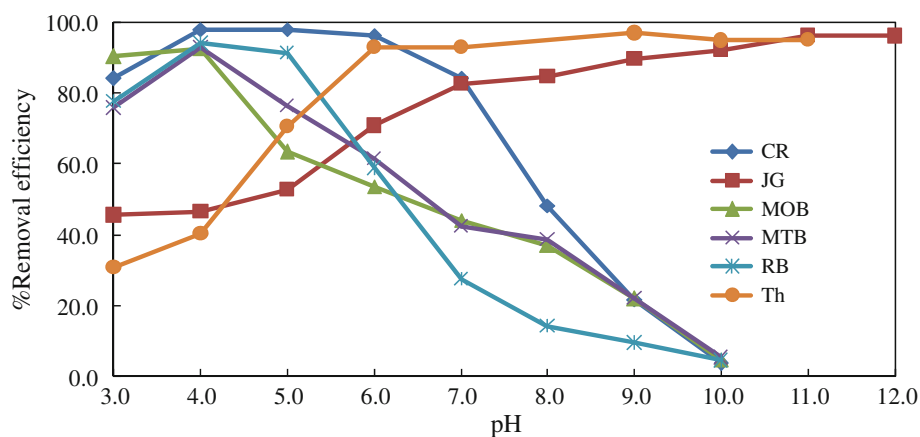

Table 1 Adsorption kinetics model rate constant for investigated dyes adsorption on MMAC

Temperature (K)	Pseudo-second order					Pseudo-first order			
	$q_{e,exp}$ (mg g^{-1})	$q_{e,cal}$ (mg g^{-1})	$k_2 \times 10^{-3}$ (g mg^{-1} h^{-1})	Corr. coeff.	RMS	$q_{e,cal}$ (mg g^{-1})	k_1 (h^{-1})	Corr. coeff.	RMS
MTB									
298	38.76	36.41	12.98	0.991	1.51	32.31	0.308	0.988	1.77
308	18.69	24.24	35.57	0.988	1.09	22.68	0.375	0.985	1.24
318	17.65	17.36	78.37	0.989	0.85	17.45	0.405	0.998	0.43
328	15.79	16.73	124.96	0.998	0.39	15.67	0.447	0.988	0.87
CR									
298	111.10	130.85	0.06	0.998	0.53	75.37	0.013	0.998	0.55
308	90.90	69.57	0.71	0.994	1.30	50.15	0.059	0.993	1.50
318	71.43	60.87	1.46	0.987	1.29	50.13	0.068	0.981	1.55
328	28.17	14.86	6.52	0.999	0.00	12.13	0.004	0.995	0.01
MOB									
298	42.49	43.31	8.17	0.999	0.39	30.77	0.161	0.979	1.67
308	37.90	37.32	13.06	0.997	0.63	30.85	0.374	0.989	1.29
318	36.31	35.87	5.82	0.994	0.91	34.30	0.277	0.995	0.91
328	33.20	32.82	23.89	0.997	0.66	38.09	0.245	0.999	0.51
RB									
298	47.62	48.27	5.89	0.998	0.81	36.61	0.083	0.995	0.51
308	44.49	42.61	11.07	0.991	1.37	42.65	0.198	0.996	1.08
318	44.05	40.20	15.66	0.995	1.09	38.92	0.284	0.978	2.18
328	40.48	38.13	2.96	0.995	0.44	37.28	0.328	0.988	1.62
JG									
298	256.41	252.53	24.71	0.999	1.25	249.98	0.711	0.999	1.81
308	250.68	250.96	25.46	0.999	0.34	248.48	0.744	0.999	0.50
318	250.00	250.56	26.37	0.999	0.31	248.28	0.761	0.999	0.41
328	250.00	250.32	29.81	0.999	0.00	247.61	0.852	0.999	0.81
Th									
298	285.71	287.28	0.66	0.997	5.17	232.39	0.159	0.994	6.79
308	256.41	255.43	1.85	0.999	2.73	237.68	0.279	0.998	4.08
318	263.16	260.86	2.04	0.999	1.45	240.20	0.308	0.996	6.19
328	258.73	257.29	6.67	0.999	2.23	246.31	0.541	0.999	0.39

Adsorption kinetics

Kinetic models are used to examine the rate of the adsorption process and the potential rate controlling step. In the present work, the kinetic data obtained from batch studies have been analyzed using pseudo-first order [30] and pseudo-second order models [31].

Temperature is an important factor governing the sorption process. The effect of temperature on the adsorption of dyes by MMAC was studied from 298 to 328 K at $C_0 = 20.0$ mg L^{-1} and a MMAC loading = 0.5 g L^{-1}. An increase in the temperature resulted in a decrease in dye adsorption capacity indicating the process to be exothermic (Table 1) as it is expected [37].

The time required to reach sorption equilibrium was increased by decreasing the temperature. This may be due to the increasing mobility of the dye molecules and

increasing number of active sites for the adsorption with the increasing temperature [38], and this may be due to the higher rate of diffusion of dye ions onto the MMAC particles surface at higher temperatures [39].

To evaluate the kinetics of the adsorption process, the pseudo-first order and pseudo-second order models were tested to interpret the experimental data. The values of k_1 and q_e, at the temperatures evaluated experimentally, were calculated using the slope and intercept of plots of log $(q_e - q_t)$ versus t (Table 1). The pseudo-second order adsorption parameters $q_{e,cal}$ and k_2 were determined by plotting t/q_t versus t (Table 1).

The best fit among the kinetic models is assessed by linear coefficient of determination (r^2) and non-linear Chi-square (χ^2) test. The Chi-square test measures the difference between the experimental and model data. The mathematical form of this test statistic can be expressed as:

$$\chi^2 = \sum \frac{(q_{e,exp} - q_{e,cal})^2}{q_{e,cal}} \tag{3}$$

where $q_{e,exp}$ is the experimental equilibrium capacity data and $q_{e,cal}$ is the equilibrium capacity from a model. If data from the model are similar to experimental data, χ^2 will be small and if they differ, χ^2 will be large.

Fitted equilibrium adsorption capacities are similar at each temperature (for each dye) and in a close agreement with those observed experimentally. Furthermore, the correlation coefficients for the pseudo-second order

Table 2 The χ^2 values for pseudo-first order and pseudo-second order models

Dye	Pseudo-second order	Pseudo-first order
MTB	1.993	1.480
CR	17.34	80.31
MOB	0.03	6.82
RB	0.60	4.34
JG	0.06	0.21
Th	0.04	16.52

Table 3 Isotherm parameters for various two and three parameters adsorption isotherms for the adsorption of dyes onto MMAC at 25.0 °C

Isotherm models	Parameters	Dyes					
		CR	RB	MTB	MOB	JG	Th
Sips	q_m (mg g^{-1})	108.6	122.1	165.8	190.5	573.9	306.1
	k_s	0.26	0.22	0.15	0.15	0.18	0.11
	$1/n$	1.48	0.62	0.62	1.92	1.28	1.57
	r^2	0.989	0.987	0.991	0.998	0.992	0.998
	RMS	5.52	6.02	7.64	4.71	25.42	5.72
Redilch–Peterson	k_R	19.8	70.1	18.8	16.7	72.8	20.4
	α_R	0.13	0.98	0.07	0.03	0.08	0.02
	β	1.057	0.91	1.08	1.18	1.10	1.18
	r^2	0.986	0.987	0.990	0.989	0.990	0.992
	RMS	6.25	6.02	7.78	10.11	28.63	13.08
Langmuir	k_L	0.19	0.47	0.13	0.10	0.14	0.76
	q_m (mg g^{-1})	116.1	104.6	174.6	213.4	612.9	343.8
	r^2	0.983	0.974	0.986	0.976	0.986	0.981
	RMS	6.26	7.79	8.21	13.62	30.02	18.55
Freundlich	k_f	35.2	40.7	53.1	48.2	120.9	59.7
	$1/n$	0.25	0.21	0.24	0.30	0.34	0.34
	r^2	0.892	0.952	0.921	0.882	0.906	0.884
	RMS	15.97	10.45	19.96	30.15	78.61	46.29

kinetics model fits are much higher than the correlation coefficients derived from pseudo-first order model fits. Given the good agreement between model fit and experimentally observed equilibrium adsorption capacity in addition to the large correlation coefficients, this suggests that the investigated dyes adsorption followed pseudo-second order kinetics and dyes ions were adsorbed onto the MMAC surface via chemical interaction.

The lower χ^2 values (Table 2) for the pseudo-second order model also suggests that dyes adsorption onto MMAC particles followed the pseudo-second order kinetics. The pseudo-first order model exhibited higher χ^2 values, suggesting poor pseudo-first order fit to the data for the dyes adsorption on MMAC.

Adsorption isotherms

In order to describe the uptake of dyes by adsorbent, the isotherms data were analyzed using four models. The two and three parameter models, namely Langmuir [33], Freundlich [32], Sips [35] and Redilch–Peterson [34]
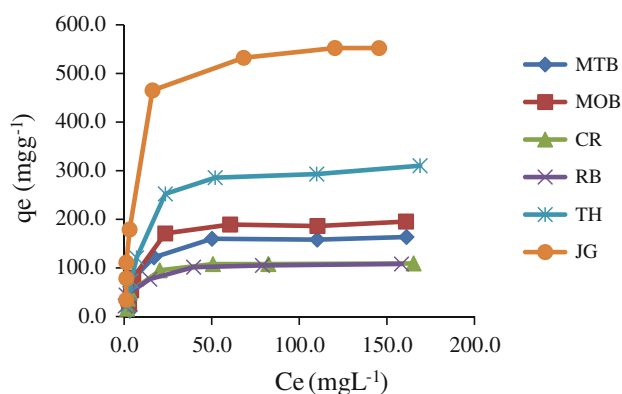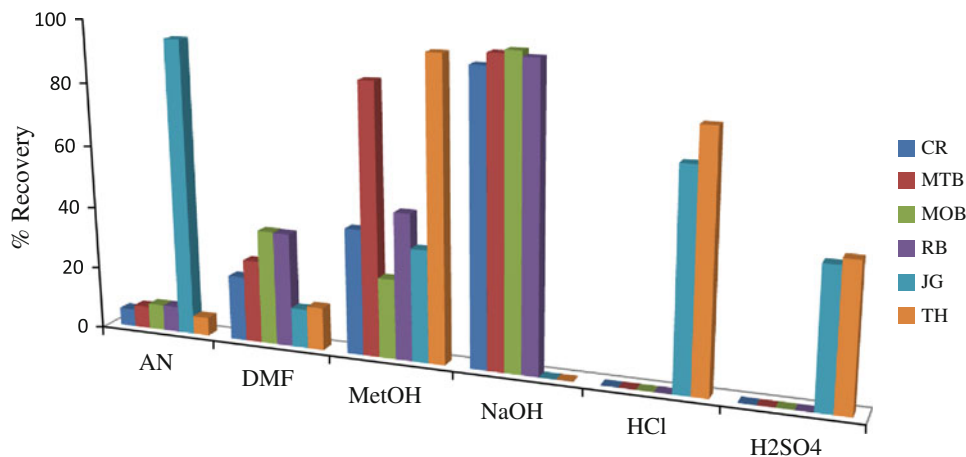

Fig. 6 Isotherm plots for adsorption of investigated dyes on the MMAC

equations have been applied to evaluate the fit by isotherm for the adsorption of dyes. And after the equilibrium adsorption data were fitted with the different isotherm models, the fitting parameter values are summarized in Table 3 and Fig. 6 shows the experimental results. The higher correlation coefficient and lower RMS factors of Sips model indicate that this model gives a better fit to the experimental data of dye–MMAC system.

Desorption and reuse studies

In order to evaluate the possibility of regeneration and the reuse of MMAC adsorbent, desorption experiments have been performed. Dye desorption from the MMAC was conducted by washing the dyes loaded on MMAC using 2.0 mL of pure methanol (MeOH), N,N-dimethyl formamide (DMF), sodium hydroxide aqueous solution (0.1 M) and acetonitrile (AN) for anionic dyes and pure methanol, acetonitrile, hydrochloride acid solution (0.01 M) and sulfuric acid (0.01 M) for cationic dyes. For this purpose, 2.0 mL of eluent was added to 0.01 g of dye-loaded MMAC in a beaker. The MMAC was collected magnetically from the solution. The concentration of dyes in the desorbed solution was measured spectrophotometrically. The results are given in Fig. 7. The results show that 0.1 M sodium hydroxide aqueous solution and methanol were effective eluents for desorption of the anionic and cationic dyes, respectively. Also acetonitrile desorbed CR efficiently. It was notable that the equilibrium of desorption was achieved within about 10 min, which was fast, similar to the adsorption equilibrium. This was due to the absence of internal diffusion resistance. After elution of the adsorbed dyes, the adsorbent was washed with DDW and vacuum dried at 25 °C overnight and reused for dye removal. The reusability of the sorbent was at least five cycles without any loss in its sorption behavior. Therefore, the MMAC can be a good reusable and economical sorbent.

Fig. 7 Regeneration of MMAC using different eluents

Table 4 Comparison of the calculated capacity factor for some synthetic adsorbents with MMAC

Adsorbent	Dye						Reference
	CR	RB	MTB	MOB	Th	JG	
SDS-γ-Fe$_2$O$_3$	–	–	–	–	200	172.4	[10]
MMMWCNTS	–	–	–	–	36.4	250	[28]
m-Cell/Fe$_3$O$_4$/ACCs	66.09	–	–	–	–	–	[40]
Bael shell carbon	98.03	–	–	–	–	–	[41]
Pd-NP-AC	76.923	–	–	–	–	–	[42]
Ag-NP-AC	66.667	–	–	–	–	–	[42]
MMAC	108.6	111.2	198.4	245.7	335.6	584.1	This study

In Table 4, we compared the ability of our inexpensive adsorbent with other adsorbents in removal of dyes from aqueous solutions. The results show that MMAC is a better adsorbent compared to some of the adsorbents.

Conclusion

Removal of cationic and anionic dyes from aqueous solutions onto MMACs surface was carried out at different temperatures. The experimental conditions of maximum adsorption of the dyes were optimized. It was observed that, under the optimized conditions, up to 98 % of dyes can be removed from the solution onto the MMAC surface. The prepared magnetic adsorbent can be well dispersed into the water and be easily separated magnetically from the medium after adsorption. The rapid adsorption rate is mainly attributed to the activated carbon structure and functional groups on the adsorbent providing large surface area and good affinity for the facile and fast adsorption of dye molecules. The adsorption data were well fitted by the Sips isotherm. As the calculated capacity factors of MMAC show, it is a very good adsorbent for removing cationic and anionic dyes and its affinity to cationic dyes was very much higher than the anionic dyes. The results of this study forecast that such magnetite-modified activated carbon can be very well recommended for wastewater treatments and controlling environmental pollution.

References

1. V.K. Gupta, L. Suhas, J. Environ. Manag. **90**, 2313 (2009)
2. Q. Husain, Crit. Rev. Biotechnol. **26**, 201 (2006)
3. F.I. Hai, K. Yamamoto, K. Fukushi, Crit. Rev. Environ. Sci. Technol. **37**, 315 (2007)
4. J.S. Bae, H.S. Freeman, Dyes Pigments **73**, 81 (2007)
5. R.M. Christie, *Environmental Aspects of Textile Dyeing* (Woodhead, Boca Raton, 2007)
6. K.L. Hatch, H.I. Maibach, Text. Chem. Color. **1**, 53 (1999)
7. H.S. Rai, M.S. Bhattacharyya, J. Singh, T.K. Bansal, P. Vats, U.C. Banerjee, Crit. Rev. Environ. Sci. Technol. **35**, 219 (2005)
8. T. Robinson, B. Chandran, P. Nigam, Water Res. **36**, 2824 (2002)
9. R.C. Bansal, M. Goyal, *Activated Carbon Adsorption* (Taylor & Francis Group, Boca Raton, 2005)
10. A. Afkhami, M. Tehrani, H. Bagheri, Desalination **263**, 240 (2010)
11. A. Afkhami, R. Moosavi, J. Hazard. Mater. **174**, 398 (2010)
12. K. Imamura, E. Ikeda, T. Nagayasu, T. Sakiyama, K. Nakanishi, J. Colloid Interface Sci. **245**, 50 (2002)
13. B.G. Linsen, *Physical and Chemical Aspects of Adsorbents and Catalysts* (Academic Press, London, 1970)
14. C. Tien, *Adsorption Calculations and Modeling* (Butterworth-Heinemann, Boston, 1994)
15. Y.H. Huang, C.L. Hsueh, C.P. Huang, L.C. Su, C.Y. Chen, Sep. Purif. Technol. **55**, 23 (2007)
16. F. Alexander, G. McKay, Kinetics of removal of basic dye from effluent using silica gel. Chem. Eng. London, 243 (1977)
17. X. Yuan, S.P. Zhuo, W. Xing, H.Y. Cui, X.D. Dai, X.M. Liu, Z.F. Yan, J. Colloid Interface Sci. **310**, 83 (2007)
18. M.A. Lillo-Rodenas, J.P. Marco-Lozar, D. Cazorla-Amoros, A. Linares-Solano, J. Anal. Appl. Pyrolysis **80**, 166 (2007)
19. T. Madrakian, A. Afkhami, M.A. Zolfigol, M. Ahmadi, N. Koukabi, Nano-Micro Lett. **4**, 57 (2012)
20. P.J.M. Carrott, M.M.L. Ribeiro Carrott, R.A. Roberts, Colloids Surf. **58**, 385 (1991)
21. Y. Al-Degs, M.A.M. Khraisheh, S.J. Allen, M.N.A. Ahmad, Sep. Sci. Technol. **36**, 91 (2001)
22. F.A. Di Giano, A.S. Natter, J. Water Poll. Control Fed. **49**, 235 (1977)
23. C. Pelekani, V.L. Snoeyink, Carbon **38**, 1423 (2000)
24. J.J. Porter, Water Wastes Eng. **9**, A8 (1972)
25. G. McKay, J. Chem. Technol. Biotechnol. **32**, 759 (1982)
26. G.M. Walker, L.R. Weatherley, Water Res. **33**, 1895 (1999)
27. Y. Al-Degs, M.A.M. Khraisheh, S.J. Allen, M.N. Ahmad, Water Res. **34**, 927 (2000)
28. T. Madrakian, A. Afkhami, M. Ahmadi, H. Bagheri, J. Hazard. Mater. **196**, 109 (2011)
29. P. Panneerselvam, N. Morad, K.A. Tan, J. Hazard. Mater. **186**, 160 (2011)
30. S. Lagergren, Kungliga Svenska Vetenkapsaka demiens. Handlingar **24**, 1 (1898)
31. Y.S. Ho, G. Mckay, Process Biochem. **34**, 451 (1999)
32. H.M.F. Freundlich, Z. Phys. Chem. **57**, 385 (1906)
33. I. Langmuir, J. Am. Chem. Soc. **38**, 2221 (1916)
34. O. Redlich, D.L. Peterson, J. Phys. Chem. **63**, 1024 (1959)
35. R. Sips, On the structure of a catalyst surface. J. Chem. Phys. **16**, 490 (1948)
36. L.C.A. Oliveira, R.V.R.A. Rios, J.D. Fabris, K. Sapag, V.K. Gargc, R.M. Lago, Appl. Clay Sci. **22**, 169 (2003)
37. G. Jegadeesan, K. Mondal, S.B. Lalvani, Environ. Prog. **24**, 289 (2005)
38. S. Dawood, T.K. Sen, Water Res. **46**, 1933 (2012)

39. Y. Yu, Y.Y. Zhuang, Z.H. Wang, J. Colloid Interface Sci. **242**, 288 (2001)
40. H.Y. Zhu, Y.Q. Fu, R. Jiang, J.H. Jiang, L. Xiao, G.M. Zeng, S.L. Zhao, Y. Wang, Chem. Eng. J. **173**, 494 (2011)
41. R. Ahmad, R. Kumar, Appl. Surface Sci. **257**, 1628 (2010)
42. M. Ghaedi, M. Nejati Biyareh, S. Nasiri Kokhdan, S. Shamsaldini, R. Sahraei, A. Daneshfar, S. Shahriyar, Materials Sci. Eng. C **32**, 725 (2012)